Enhanced spin-dependent parity-nonconservation effect in the $7s\ ^2S_{1/2} \rightarrow 6d\ ^2D_{5/2}$ transition in Fr: A possibility for unambiguous detection of the nuclear anapole moment

B. K. Sahoo,[1,*] T. Aoki,[2] B. P. Das,[3] and Y. Sakemi[4]

[1]*Theoretical Physics Division, Physical Research Laboratory, Ahmedabad-380009, India*

[2]*Institute of Physics, Graduate School of Arts and Sciences, University of Tokyo, Tokyo 153-8902, Japan*

[3]*International Education and Research Center of Science and Department of Physics, Tokyo Institute of Technology, 2-1-2-1-H86 Ookayama Meguro-ku, Tokyo 152-8550, Japan*

[4]*Cyclotron and Radioisotope Center, Tohoku University, Sendai, Miyagi 980-8578, Japan*

(Received 8 December 2015; revised manuscript received 19 February 2016; published 30 March 2016)

Employing the relativistic coupled-cluster method, comparative studies of the parity nonconserving electric dipole amplitudes for the $7s\ ^2S_{1/2} \rightarrow 6d\ ^2D_{5/2}$ transitions in ^{210}Fr and ^{211}Fr isotopes have been carried out. It is found that these transition amplitudes, sensitive only to the nuclear spin-dependent effects, are enhanced substantially owing to the very large contributions from the electron core-polarization effects in Fr. This translates to a relatively large and, in principle, measurable induced light shift, which would be a signature of nuclear spin-dependent parity nonconservation that is dominated by the nuclear anapole moment in a heavy atom like Fr. A plausible scheme to measure this quantity using the Cyclotron and Radioisotope Center (CYRIC) facility at Tohoku University has been outlined.

DOI: 10.1103/PhysRevA.93.032520

I. INTRODUCTION

The study of parity nonconservation (PNC) effects in atomic systems, which involve the interplay between the weak and electromagnetic interactions [1], has important implications for atomic physics, nuclear physics, and particle physics [2–4]. For example, it could (i) provide hints for the possible existence of new physics beyond the standard model (SM) of particle interactions [5], (ii) probe the existence of the nuclear anapole moment (NAM), which is presumed to be a fundamental property of an atomic nucleus [3,6,7], and (iii) test the role of the electron correlation effects in a parity-nonconserving electric dipole transition amplitude that depends on the region near and far from the nucleus [8]. A high-precision PNC measurement for the $6s\ ^2S_{1/2} \rightarrow 7s\ ^2S_{1/2}$ transition in Cs has yielded a result that is in good agreement with the SM [9,10], and it has also led to the observation of its NAM with an accuracy of 15% [9]. However, it is at variance with the results of the shell model and the nucleon-nucleon scattering experiments [11,12]. It is, therefore, imperative to search for NAMs in other systems. Because of this reason, a PNC measurement was carried out on the $6s^2\ ^1S_0 \rightarrow 5d6s\ ^3D_1$ transition in Yb [13]. It is indeed desirable to observe an NAM unambiguously in an atomic system. Fortson has made an important proposal to measure PNC using a single trapped ion [14] based on the observation of the PNC-induced light shift, which arises due to the interference of the parity nonconserving electric dipole and the electric quadrupole (E2) amplitudes of a transition such as the $6s\ ^2S_{1/2} \rightarrow 5d\ ^2D_{3/2}$ transition in Ba^+. Though the choice of a single ion would limit the statistical uncertainty, it can be partly compensated by selecting a transition such that the upper state has a long lifetime like the above transition in Ba^+ [14], and furthermore, the large storage time in a trap contributes to enhancing the sensitivity of the scheme proposed by Fortson. As a consequence, the forbidden low-lying S-D transitions in the singly charged Ba [14–18], Yb [18–20], and Ra [17,18,21–23] ions have been considered for the PNC studies. In fact, it has also been pointed out that existence of the NAM can be unambiguously inferred from the measurements of the nuclear spin-dependent (NSD) PNC in the S-$D_{5/2}$ transitions of these ions using the techniques similar to the observation of the light shift techniques in Refs. [15,17]. The major disadvantage of these transitions is that their $E1^{\rm PNC}$ amplitudes are small [15,17,18]. The measurement of the NAM of Fr has been proposed in Refs. [24,25] by considering the hyperfine transitions of the ground state of that atom. In this article we demonstrate that the $E1^{\rm PNC}$ amplitude for the $7s\ ^2S_{1/2} \rightarrow 6d\ ^2D_{5/2}$ transition in Fr, which arises only from the NSD interaction, is enhanced relative to the same transition in the heavy ions mentioned above. Thus, the PNC light shift for this transition will also be enhanced. In this case, the loss in the statistical uncertainty due to relatively shorter lifetime of the $6d\ ^2D_{5/2}$ state of Fr can be compensated for by using a large number of atoms. Thus, if the above PNC amplitude can be measured successfully, it would constitute an unambiguous signature of the NAM.

II. THEORY AND METHOD OF CALCULATIONS

We employ the relativistic coupled cluster (RCC) theory in the singles, doubles, and important partial triples excitations approximation ($\rm CCSD_{t3}$ method) [28,29] to evaluate the NSD PNC amplitudes corresponding to the transitions between different hyperfine levels of the ground state and the $7s\ ^2S_{1/2} \rightarrow 8s\ ^2S_{1/2}$, $7s\ ^2S_{1/2} \rightarrow 6d\ ^2D_{3/2}$, and $7s\ ^2S_{1/2} \rightarrow 6d\ ^2D_{5/2}$ transitions of ^{210}Fr, ^{211}Fr, and ^{223}Fr. The principle of the experiment to observe their signature is given later, and it involves the measurement of the PNC-induced light shift of the $7s\ ^2S_{1/2} \rightarrow 6d\ ^2D_{5/2}$ transition in ^{210}Fr. In addition, we also present results for the other three transitions and for those corresponding to ^{211}Fr and ^{223}Fr isotope for three specific reasons. First, the calculations of the NSD PNC amplitudes

*bijaya@prl.res.in

in some of these transitions for ^{211}Fr and ^{223}Fr have already been reported using different relativistic many-body methods [18,26,27], and it is instructive to compare their results with those we have obtained. Second, our calculations for ^{211}Fr could be useful for another experiment involving ground state hyperfine transitions (e.g., Refs. [24,25]). Third, the nuclear spin I of ^{210}Fr is an integer ($I = 6$) while I of ^{211}Fr and ^{223}Fr are half-integers ($I = 9/2$ and $I = 3/2$), which can be appropriately used in different experimental setups.

The Hamiltonian due to the NSD PNC interaction is given by [7]

$$H_{\rm PNC}^{\rm NSD} = \frac{G_F}{\sqrt{2}} \mathcal{K}_W \boldsymbol{\alpha} \cdot \mathbf{I}\, \rho_{\rm nuc}(r), \tag{1}$$

where G_F is the Fermi constant, $\rho_{\rm nuc}$ is the nuclear density, and $\boldsymbol{\alpha}$ is the Dirac matrix. In the above expression the dimensionless quantity $\mathcal{K}_W$ is related to NAM. The $E1^{\rm PNC}$ amplitude due to the NSD interaction between the hyperfine states $|F_f, M_f\rangle$ and $|F_i, M_i\rangle$ is given by

$$E1^{\rm PNC}_{M_f M_i} = (-1)^{F_f - M_f} \begin{pmatrix} F_f & 1 & F_i \\ -M_f & q & M_i \end{pmatrix} \mathcal{Y}, \tag{2}$$

where $q = -1$, 0 or 1 depends on the choice of the M values. For the theoretical purpose, enhancement in the $E1^{\rm PNC}$ is estimated by calculating the reduced matrix element $\mathcal{Y}$ given by [18,26,27]

$$\begin{aligned} \mathcal{Y} = \eta \Bigg(& \sum_{k \neq i} (-1)^{j_i - j_f + 1} \frac{\langle J_f || D || J_k \rangle \langle J_k || K^1 || J_i \rangle}{E_i - E_k} \\ & \times \begin{Bmatrix} F_f & F_i & 1 \\ J_k & J_f & I \end{Bmatrix} \begin{Bmatrix} I & I & 1 \\ J_k & J_i & F_i \end{Bmatrix} \\ & + \sum_{k \neq f} (-1)^{F_i - F_f + 1} \frac{\langle J_f || K^1 || J_k \rangle \langle J_k || D || J_i \rangle}{E_f - E_k} \\ & \times \begin{Bmatrix} F_f & F_i & 1 \\ J_i & J_k & I \end{Bmatrix} \begin{Bmatrix} I & I & 1 \\ J_k & J_f & F_f \end{Bmatrix} \Bigg), \end{aligned} \tag{3}$$

where $\eta = \sqrt{(I+1)(2I+1)(2F_i+1)(2F_f+1)/I}$ and E are the energies of the respective states. The above expression is derived by rewriting $H_{\rm PNC}^{\rm NSD} = \frac{1}{|I|} \sum_q (-1)^q I_q^1 K_{-q}^1$. We determine these quantities in a sum-over-states approach by calculating the reduced matrix elements of the D and K operators. However, we include contributions explicitly only from the $7P - 11P$ low-lying states obtained using the CCSD$_{\rm t3}$ method. This method has already been applied earlier to evaluate both the hyperfine structure constants and radiative transition matrix elements of the Fr isotopes accurately [28,29]. The CCSD$_{\rm t3}$ matrix elements of both the electric dipole (E1) and K^1 operators involving these P states are quoted in Table I.

TABLE I. Reduced matrix elements of the dipole operator D in atomic unit (ea_0) and of the operator K^1 in $i\mathcal{K}_W \times 10^{-11}$ among the S-P and S-D transitions in Fr. Here $\mathcal{K}_W$ is the weak coupling coefficient.

J_f state	J_i state	$\langle J_f \|\| D \|\| J_i \rangle$	$\langle J_f \|\| K^1 \|\| J_i \rangle$
$7p\ ^2P_{1/2}$	$7s\ ^2S_{1/2}$	4.26	25.03
$8p\ ^2P_{1/2}$	$7s\ ^2S_{1/2}$	0.34	14.64
$9p\ ^2P_{1/2}$	$7s\ ^2S_{1/2}$	−0.11	−9.93
$10p\ ^2P_{1/2}$	$7s\ ^2S_{1/2}$	0.06	7.39
$11p\ ^2P_{1/2}$	$7s\ ^2S_{1/2}$	−0.04	−5.92
$7p\ ^2P_{3/2}$	$7s\ ^2S_{1/2}$	5.98	2.54
$8p\ ^2P_{3/2}$	$7s\ ^2S_{1/2}$	0.95	1.02
$9p\ ^2P_{3/2}$	$7s\ ^2S_{1/2}$	0.44	0.61
$10p\ ^2P_{3/2}$	$7s\ ^2S_{1/2}$	0.28	0.45
$11p\ ^2P_{3/2}$	$7s\ ^2S_{1/2}$	0.18	0.32
$8s\ ^2S_{1/2}$	$7p\ ^2P_{1/2}$	−4.27	−12.96
$8s\ ^2S_{1/2}$	$8p\ ^2P_{1/2}$	10.08	−6.60
$8s\ ^2S_{1/2}$	$9p\ ^2P_{1/2}$	−1.00	4.53
$8s\ ^2S_{1/2}$	$10p\ ^2P_{1/2}$	0.42	−3.38
$8s\ ^2S_{1/2}$	$11p\ ^2P_{1/2}$	0.24	2.71
$8s\ ^2S_{1/2}$	$7p\ ^2P_{3/2}$	7.53	−0.73
$8s\ ^2S_{1/2}$	$8p\ ^2P_{3/2}$	−13.31	−0.60
$8s\ ^2S_{1/2}$	$9p\ ^2P_{3/2}$	−2.26	−0.36
$8s\ ^2S_{1/2}$	$10p\ ^2P_{3/2}$	−1.09	−0.26
$8s\ ^2S_{1/2}$	$11p\ ^2P_{3/2}$	−0.63	−0.18
$6d\ ^2D_{3/2}$	$7p\ ^2P_{1/2}$	−7.45	2.60
$6d\ ^2D_{3/2}$	$8p\ ^2P_{1/2}$	2.75	0.49
$6d\ ^2D_{3/2}$	$9p\ ^2P_{1/2}$	−0.83	−0.22
$6d\ ^2D_{3/2}$	$10p\ ^2P_{1/2}$	−0.45	0.14
$6d\ ^2D_{3/2}$	$11p\ ^2P_{1/2}$	−0.29	−0.10
$6d\ ^2D_{3/2}$	$7p\ ^2P_{3/2}$	−3.44	−0.17
$6d\ ^2D_{3/2}$	$8p\ ^2P_{3/2}$	0.88	−0.45
$6d\ ^2D_{3/2}$	$9p\ ^2P_{3/2}$	0.28	−0.35
$6d\ ^2D_{3/2}$	$10p\ ^2P_{3/2}$	0.15	−0.28
$6d\ ^2D_{3/2}$	$11p\ ^2P_{3/2}$	0.09	−0.21
$6d\ ^2D_{5/2}$	$7p\ ^2P_{3/2}$	−10.53	−5.10
$6d\ ^2D_{5/2}$	$8p\ ^2P_{3/2}$	2.83	−2.01
$6d\ ^2D_{5/2}$	$9p\ ^2P_{3/2}$	0.90	−1.27
$6d\ ^2D_{5/2}$	$10p\ ^2P_{3/2}$	0.48	−0.91
$6d\ ^2D_{5/2}$	$11p\ ^2P_{3/2}$	0.29	−0.68

III. RESULTS AND DISCUSSION

Using the matrix elements given in Table I and experimental energy values listed in the National Institute of Science and Technology (NIST) database [30], we evaluate the contribution to $\mathcal{Y}$ for all possible hyperfine levels among the ground, $8s\ ^2S_{1/2} \rightarrow 7s\ ^2S_{1/2}$, $6d\ ^2D_{3/2} \rightarrow 7s\ ^2S_{1/2}$, and $6d\ ^2D_{5/2} \rightarrow 7s\ ^2S_{1/2}$ transitions of ^{210}Fr, ^{211}Fr, and ^{223}Fr isotopes. We present these results in Table II. To understand roles of the initial perturbed and final perturbed states in the accurate evaluation of results, we give explicitly the results from the initial perturbed state as "Initial" and from the final perturbed state as "Final" in the same table. Again, we have also estimated contributions from the core valence correlations and the higher level excited states using a second order perturbation theory [MBPT(2) method]. These quantities are also given explicitly as "Core" and "Tail" contributions in the table. As can be seen magnitudes of both the "Core" and "Tail" contributions are extremely small; hence obtaining them using the MBPT(2) method seems to be reasonable. As noticed from Table II, the "Final" contributions are large than the "Initial" contributions for the $S - S$ and S-$D_{5/2}$ transitions, while this trend is the other way around for the S-$D_{3/2}$ transitions. In fact, the "Final" contributions in the S-$D_{5/2}$ transitions are as large as the corresponding contributions in the S-S transitions. The

TABLE II. Contributions to the reduced matrix elements of $\mathcal{Y}$ in $iea_0\mathcal{K}_W \times 10^{-11}$ from the final perturbed state (Final) and initial perturbed state (Initial) considering intermediate states up to the $11P$ states in the corresponding transitions of ^{210}Fr, ^{211}Fr, and ^{223}Fr. Contributions from the core valence and higher level excited states are given as "Core" and "Tail", respectively. The total results are compared against the values reported in.

			This work					Other
$J_f \rightarrow J_i$	F_f	F_i	Final	Initial	Core	Tail	Total	works
^{210}Fr ($I = 6$)								
$7s\ ^2S_{1/2} \rightarrow 7s\ ^2S_{1/2}$	11/2	13/2	−2.907	−2.414	−0.172	−0.035	−5.529	
$8s\ ^2S_{1/2} \rightarrow 7s\ ^2S_{1/2}$	11/2	11/2	1.284	−0.545	−0.002	0.008	0.745	
	13/2	11/2	2.029	0.893	−0.077	−0.063	1.847	
	11/2	13/2	2.321	0.401	−0.077	−0.062	2.026	
	13/2	13/2	1.389	−0.589	−0.002	−0.008	0.789	
$6d\ ^2D_{3/2} \rightarrow 7s\ ^2S_{1/2}$	9/2	11/2	−0.089	3.341	0.127	−0.085	3.294	
	11/2	11/2	−0.480	−3.205	−0.118	0.078	−3.725	
	13/2	11/2	0.905	2.631	0.093	−0.062	3.568	
	11/2	13/2	−0.853	−1.832	−0.063	0.042	−2.706	
	13/2	13/2	0.700	2.800	0.102	−0.068	3.531	
	15/2	13/2	0.096	−3.622	−0.138	0.092	−3.572	
$6d\ ^2D_{5/2} \rightarrow 7s\ ^2S_{1/2}$	9/2	11/2	−1.555	0.233	∼0.0	∼0.0	−1.323	
	11/2	11/2	1.929	−0.288	∼0.0	∼0.0	1.641	
	13/2	11/2	−1.652	0.247	∼0.0	∼0.0	−1.405	
	11/2	13/2	−1.209	0.181	∼0.0	∼0.0	−1.028	
	13/2	13/2	2.090	−0.312	∼0.0	∼0.0	1.777	
	15/2	13/2	−2.503	0.374	∼0.0	∼0.0	−2.129	
^{211}Fr ($I = 9/2$)								
$7s\ ^2S_{1/2} \rightarrow 7s\ ^2S_{1/2}$	4.0	5.0	−2.677	−2.101	−0.153	−0.031	−4.962	−5.287[a], −4.9[b]
$8s\ ^2S_{1/2} \rightarrow 7s\ ^2S_{1/2}$	4.0	4.0	1.133	−0.481	−0.002	0.007	0.657	0.687[a]
	5.0	4.0	1.782	0.488	−0.069	−0.056	2.145	2.050[a]
	4.0	5.0	2.123	0.343	−0.069	−0.056	2.342	2.258[a]
	5.0	5.0	1.255	0.040	−0.002	0.007	0.728	0.761[a]
$6d\ ^2D_{5/2} \rightarrow 7s\ ^2S_{1/2}$	3.0	4.0	−1.256	0.188	∼0.0	∼0.0	−1.068	−0.243[c]
	4.0	4.0	1.685	−0.252	∼0.0	∼0.0	1.433	0.326[c]
	5.0	4.0	−1.531	0.229	∼0.0	∼0.0	−1.302	−0.296[c]
	4.0	5.0	−1.016	0.152	∼0.0	∼0.0	−0.864	−0.197[c]
	5.0	5.0	1.875	−0.280	∼0.0	∼0.0	1.594	0.363[c]
	6.0	5.0	−2.365	0.354	∼0.0	∼0.0	−2.011	−0.458[c]
^{223}Fr ($I = 3/2$)								
$6d\ ^2D_{3/2} \rightarrow 7s\ ^2S_{1/2}$	0.0	1.0	−0.041	1.509	0.060	−0.040	1.489	1.816[c]
	1.0	1.0	−0.157	−2.427	−0.093	0.060	−2.617	−2.928[c]
	2.0	1.0	0.598	2.509	0.093	−0.060	3.140	3.033[c]
	1.0	2.0	−0.476	−0.732	−0.027	0.013	−1.221	−0.891[c]
	2.0	2.0	0.623	1.554	0.053	−0.033	2.197	1.882[c]
	3.0	2.0	0.064	−2.396	−0.093	0.060	−2.365	−2.886[c]

[a]Refs. [27] (to be consistent values are divided by nuclear spin I).
[b][26].
[c][18].

main reason for this is due to large reduced matrix elements of the K^1 operator in the $6d\ ^2D_{5/2} \rightarrow np\ ^2P_{3/2}$ transitions, for the intermediate states n.

We also compare our results with the other available calculations for ^{211}Fr [18,26,27] in Table II. All these calculations start with a V^{N-1} potential, but Johnson *et al.* have employed the random phase approximation (RPA) to calculate the $\mathcal{Y}$ values only for the S-S transitions [27]. Our CCSD$_{t3}$ method contains these effects implicitly along with the core-correlation and pair-correlation effects to all orders. Nevertheless our calculations agree quite well with these RPA results, the differences mainly owing to the pair-correlation effects that are significant for the S states as seen in the studies of the hyperfine structure constants of ^{210}Fr [29]. Recently, Roberts *et al.* have calculated $\mathcal{Y}$ values for the $7s\ ^2S_{1/2} \rightarrow 6d\ ^2D_{5/2}$ transition that take into account the core-valence correlation effects using the correlation potential (CP) method and the polarization of the core electrons and interactions with the external fields using RPA. But they mention that their results can be improved after inclusion of the other higher order correlation corrections such as the double-core-polarization, structural radiation, and ladder diagrams [18]. On comparison, we find at least one order of magnitude difference between their results and ours. Our analysis shows that the extraordinarily large

core polarization effects enhance the $\langle 6d\ ^2D_{5/2}|K^1|np\ ^2P_{3/2}\rangle$ matrix elements that appear in the second term of Eq. (3), and their values become more than two times larger than the $\langle np\ ^2P_{3/2}|K^1|7s\ ^2S_{1/2}\rangle$ matrix elements, where n represents the principal quantum numbers of p orbitals. The two factors that are responsible for such enhancements are the small energy difference between the $6d\ ^2D_{5/2}$ and $7p\ ^2P_{3/2}$ states and large overlap between the valence $7s$ orbital and the occupied $p_{1/2}$ orbitals. The other factors that also play vital roles here are the large $\langle 6d\ ^2D_{5/2}|D|7p\ ^2P_{3/2}\rangle$ matrix element [$\sim$10.51(7) ea_0 [28]] and the positioning of the the $7p\ ^2P_{3/2}$ state between the $7s\ ^2S_{1/2}$ and $6d\ ^2D_{5/2}$ states. Due to the same reason, the enhancement for this transition in Fr is much larger than its isoelectronic partner Ra^+ and for the $6s\ ^2S_{1/2} \rightarrow 5d\ ^2D_{5/2}$ transition of Ba^+ [17,18]. It is also observed that $\mathcal{Y}$ values in ^{210}Fr are larger than ^{211}Fr due to its large I.

We suggest an approach similar to that proposed by Fortson [14] to measure the NSD PNC-induced light shift ($\omega^{\rm PNC}$) arising from the interference of the NSD $E1^{\rm PNC}$ and E2 amplitudes between the hyperfine states of the $7s\ ^2S_{1/2} \rightarrow 6d\ ^2D_{5/2}$ transition in ^{210}Fr. Figure 1 shows schematic diagrams of the relevant transitions for the PNC measurement and indicates that the $7s\ ^2S_{1/2} \rightarrow 6d\ ^2D_{5/2}$ transition is in the optical regime. The frequency for a transition with the same hyperfine sublevels M can be estimated using the expression [14]

$$\Delta\omega_M^{\rm PNC} \approx -\frac{{\rm Re}\sum_{M'}\left(\Omega_{MM'}^{\rm PNC*}\Omega_{MM'}^{E2}\right)}{\sqrt{\sum_{M'}|\Omega_{MM'}^{E2}|^2}}, \tag{4}$$

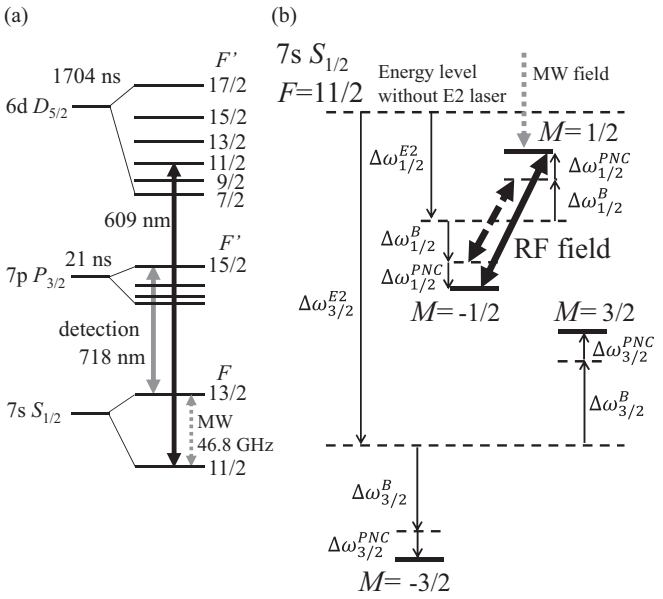

FIG. 1. Schematic energy level diagrams of ^{210}Fr. (a) Arrows indicate laser-induced transitions for observing the E2 light shifts, detecting the states, and carrying out the microwave (MW) transitions between the hyperfine levels. (b) Magnetic sublevels (shown only for $M = \pm 3/2$ and $M = \pm 1/2$) of the $F = 11/2$ level of the $7s\ ^2S_{1/2}$ state with the corresponding RF transitions. The solid and dashed arrows indicate the resonant RF transitions in the presence and absence of the PNC-induced light shift, respectively.

where $\Omega^{\rm PNC}$ and Ω^{E2} are the Rabi frequencies due to the $E1^{\rm PNC}$ and E2 amplitudes, and the summation over M' is for all possible allowed intermediate states. This will be much smaller compared to the changes in the transition frequency due to the E2 shift alone, which is given by

$$\Delta\omega_M^{E2} \approx \frac{(\omega_0 - \omega)}{2} - \sqrt{\sum_{M'}|\Omega_{MM'}^{E2}|^2} \tag{5}$$

for the respective frequencies ω_0 and ω corresponding to the transition before and after applying the laser. In the nuclear shell model, ^{210}Fr has an odd proton in the $\pi h_{9/2}$ shell and an odd neutron in the $\nu f_{5/2}$ shell. We determine $\mathcal{K}_W$ of this isotope considering the dominant contribution from the odd proton due to the NAM using the expression in natural unit [3,31]

$$\mathcal{K}_W \approx \frac{9}{10} g_p \mu_p \frac{\alpha A^{2/3}}{M_p r_0}, \tag{6}$$

where $g_p \simeq 5.0$ is the nucleon-nucleon parity-odd coupling and $\mu_p \simeq 2.8$ is the magnitude of the magnetic moment of the proton, A is the atomic number, M_p is the proton mass, and $r_0 \simeq 1.2$ fm. Considering the $\mathcal{Y}$ values from Table I, $M = 1/2$, $\mathcal{K}_W \simeq 0.568$ from the above formula, the values of the electric field and the E2 amplitude are $2 \times 10^6\ V/m$ and 39.33 ea_0^2 [28], respectively, we have estimated $\Delta\omega_M^{E2}$ and $\Delta\omega_M^{\rm PNC}$ values for different hyperfine levels of the $7s\ ^2S_{1/2} \rightarrow 6d\ ^2D_{5/2}$ transition in ^{210}Fr and presented in Table III. We find that there is significant enhancement in the PNC-induced light shift for the $F_i = 11/2 \rightarrow F_f = 11/2$ transition. The measurements of these quantities are possible using the laser-cooled ^{210}Fr atoms in an optical lattice that is being set up at the Cyclotron and Radioisotope Center at Tohoku University. We plan to irradiate two standing-wave laser fields (similar to that suggested in Ref. [14]) with wavelengths of 609 nm, which are resonant with the $7s\ ^2S_{1/2}(F = 11/2) \rightarrow 6d\ ^2D_{5/2}(F' = 11/2)$ E2 transition, as shown in the black solid arrow in Fig. 1(a). The PNC-induced light shift, which is given by Eq. (4), can be measured from the Ramsey resonance by applying the radio frequency (RF) field, as shown in Fig. 1(b), arising from two pulses separated in time. Thus, the magnetic sublevels $M = \pm 1/2$ of the $7s\ ^2S_{1/2}(F = 11/2)$ state can be shifted in this scheme by the E2 light field ($\Delta\omega_{|M|}^{E2}$), Zeeman effect ($\Delta\omega_{|M|}^{B}$) and the PNC-induced effect ($\Delta\omega_M^{\rm PNC}$); where $|M|$ in the subscripts indicate that the corresponding

TABLE III. Estimated light shifts in the hyperfine levels of the $7s\ ^2S_{1/2}(F_i) \rightarrow 6d\ ^2D_{5/2}(F_f)$ transition of ^{210}Fr due to the E2 (in MHz) and NSD PNC (in $\times 10^{-4}$ Hz) interactions with the applied electric field 2×10^6 V/m. Here we have used $\mathcal{K}_W \approx 0.568$ and E2 amplitude as 39.33 ea_0^2.

F_f	F_i	M	$\Delta\omega_{\lvert M\rvert}^{E2}/2\pi$	$\Delta\omega_M^{\rm PNC}/2\pi$
9/2	11/2	1/2	9.15	10.5
11/2	11/2	1/2	2.32	−288.4
13/2	11/2	1/2	6.41	−10.2
11/2	13/2	1/2	5.46	−5.5
13/2	13/2	1/2	1.70	289.9
15/2	13/2	1/2	7.91	10.5

shifts are independent of the sign of M. We estimate the values of $\Delta\omega^{E2}_{|M|}$ between the $M = \pm 1/2$ and $\pm 3/2$ sublevels as $\sim$1.70 MHz and $\sim$3.70 MHz, respectively, for the $7s\ ^2S_{1/2}(F = 11/2) \rightarrow 6d\ ^2D_{5/2}(F' = 11/2)$ transition. Similarly, $\Delta\omega^{B}_{1/2}/2\pi$ is ~ 0.1 MHz for a magnetic field strength of 1 G, which is much smaller than the estimated E2 light shifts. The frequency of the RF field will be resonant only with the $M = -1/2 \leftrightarrow M = 1/2$ transition. As shown in Fig. 1(b), this RF field will not induce a transition between any other magnetic sublevels. Interactions of the two-pulses with the ^{210}Fr atoms can produce the Ramsey fringes. After the application of the two pulses of the RF field, the states selective detection can be achieved from the following manner: (i) A microwave (MW) field of 46.8 GHz is applied as a π pulse, causing a transition from the $|F = 11/2, M = 1/2\rangle$ level to the $|F = 13/2, M = 1/2\rangle$ level, as shown in Fig. 1(a) and (b). (ii) Using laser to drive the transition from the $7s\ ^2S_{1/2}(F = 13/2)$ state to the $7p\ ^2P_{3/2}(F' = 15/2)$ state (718 nm optical transition) and detecting the fluorescence, representing the Ramsey fringes from this transition, can be detected by a photo multiplier tube in order to measure the final population in the $M = 1/2$ state. The RF transition mentioned earlier will not be affected by the E2 light shift fluctuation due to the amplitude noise of the laser fields but by the PNC light shifts owing to opposite signs for the $\Delta\omega^{\rm PNC}_{M}$ values for the $M = -1/2$ and $M = 1/2$ levels. Therefore, comparing the phase shifts of the Ramsey fringes in the presence and absence of the E2 laser field would yield a net shift equal to $2\Delta\omega^{\rm PNC}_{1/2}$. The uncertainty in the measurement would be restricted by the shot noise limit given by $\delta\omega/2\pi = 1/(2\pi\sqrt{\tau NT})$ [14], where τ is the separation time between the two RF pulses, N is the number of trapped atoms, and T is the total measurement time. If τ is $\sim$1704 ns, the lifetime of the $6d\ ^2D_{5/2}$ state [28], and $N = 10^4$, the number of atoms that is expected to be trapped in CYRIC, T should be more than 442 s in order to obtain the PNC-induced light shift of 0.058 Hz.

IV. CONCLUSION

We have analyzed the PNC-induced light shifts in the $7s\ ^2S_{1/2} \rightarrow 6d\ ^2D_{5/2}$ transition in ^{210}Fr and have proposed a plausible experimental scheme to measure them using the CYRIC facility. Calculations in ^{210}Fr, ^{211}Fr, and ^{223}Fr using the RCC theory showed large enhancements of the PNC amplitudes due to strong core-polarization effects. This suggests that an unambiguous observation of the NAM in Fr is possible. Our calculations of the PNC amplitudes for ^{211}Fr and ^{223}Fr could be useful if the corresponding PNC-induced light shift measurements are carried out in another facility.

ACKNOWLEDGMENTS

We would like to thank Dr. M. Mukherjee for many useful discussions on light shifts. B.K.S. thanks Prof. V. V. Flambaum for explaining the anapole moment expression. This work was supported partly by INSA-JSPS under Project No. IA/INSA-JSPS Project/2013-2016/February 28,2013/4098. Computations were carried out using the PRL Vikram-100 HPC cluster.

[1] M.-A. Bouchiat and C. Bouchiat, Rep. Prog. Phys. **60**, 1351 (1997).
[2] E. D. Commins and P. H. Bucksbaum, *Weak Interactions of Leptons and Quarks* (Cambridge University Press, Cambridge, 1983).
[3] V. V. Flambaum and I. B. Khriplovich, J. Exp. Theo. Phys. **52**, 835 (1980).
[4] J. Erler and P. Langacker, Phys. Rev. Lett. **105**, 031801 (2010).
[5] W. J. Marciano and J. L. Rosner, Phys. Rev. Lett. **65**, 2963 (1990).
[6] Ya. B. Zeldovich, Zh. Eksp. Teor. Fiz. **33**, 1531 (1957) [Sov. Phys. JETP **6**, 1184 (1957)].
[7] J. S. M. Ginges and V. V. Flambaum, Phys. Rep. **397**, 63 (2004).
[8] B. K. Sahoo, G. Gopakumar, R. K. Chaudhuri, B. P. Das, H. Merlitz, U. S. Mahapatra, and D. Mukherjee, Phys. Rev. A **68**, 040501(R) (2003).
[9] C. S. Wood *et al.*, Science **275**, 1759 (1997).
[10] S. G. Porsev, K. Beloy, and A. Derevianko, Phys. Rev. Lett. **102**, 181601 (2009).
[11] W. S. Wilburn and J. D. Bowman, Phys. Rev. C **57**, 3425 (1998).
[12] W. C. Haxton and C. E. Wieman, Ann. Rev. Nuc. Part. Sc. **51**, 261 (2001).
[13] K. Tsigutkin, D. Dounas-Frazer, A. Family, J. E. Stalnaker, V. V. Yashchuk, and D. Budker, Phys. Rev. Lett. **103**, 071601 (2009).
[14] N. Fortson, Phys. Rev. Lett. **70**, 2383 (1993).
[15] K. P. Geetha, A. D. Singh, B. P. Das, and C. S. Unnikrishnan, Phys. Rev. A **58**, R16(R) (1998).
[16] B. K. Sahoo, R. Chaudhuri, B. P. Das, and D. Mukherjee, Phys. Rev. Lett. **96**, 163003 (2006).
[17] B. K. Sahoo, P. Mandal, and M. Mukherjee, Phys. Rev. A **83**, 030502(R) (2011).
[18] B. M. Roberts, V. A. Dzuba, and V. V. Flambaum, Phys. Rev. A **89**, 012502 (2014).
[19] S. G. Porsev, M. S. Safronova, and M. G. Kozlov, Phys. Rev. A **86**, 022504 (2012).
[20] B. K. Sahoo and B. P. Das, Phys. Rev. A **84**, 010502(R) (2011).
[21] L. W. Wansbeek, B. K. Sahoo, R. G. E. Timmermans, K. Jungmann, B. P. Das, and D. Mukherjee, Phys. Rev. A **78**, 050501(R) (2008).
[22] R. Pal, D. Jiang, M. S. Safronova, and U. I. Safronova, Phys. Rev. A **79**, 062505 (2009).
[23] B. M. Roberts, V. A. Dzuba, and V. V. Flambaum, Phys. Rev. A **88**, 012510 (2013).
[24] E. Gomez, S. Aubin, G. D. Sprouse, L. A. Orozco, and D. P. DeMille, Phys. Rev. A **75**, 033418 (2007).

[25] D. Sheng, L. A. Orozco, and E. Gomez, J. Phys. B: At. Mol. Opt. Phys. **43**, 074004 (2010).
[26] S. G. Porsev and M. G. Kozlov, Phys. Rev. A **64**, 064101 (2001).
[27] W. R. Johnson, M. S. Safronova, and U. I. Safronova, Phys. Rev. A **67**, 062106 (2003).
[28] B. K. Sahoo and B. P. Das, Phys. Rev. A **92**, 052511 (2015).
[29] B. K. Sahoo, D. K. Nandy, B. P. Das, and Y. Sakemi, Phys. Rev. A **91**, 042507 (2015).
[30] http://physics.nist.gov/cgi-bin/ASD/energy1.pl.
[31] V. V. Flambaum, I. B. Khriplovich, and O. P. Sushkov, Phys. Lett. B **146**, 367 (1984).